applied sciences

MDPI

Article

Effect of Fines Content on the Compression Behavior of Calcareous Sand

Suhang Huang * and Xiaonan Gong

Research Center of Coastal and Urban Geotechnical Engineering, Zhejiang University, Hangzhou 310058, China
* Correspondence: huangsuh@zju.edu.cn

Abstract: Due to the hydraulic sorting effect in the hydraulic filling process, a fine-grained aggregate layer dominated by silty fine sand with uneven distribution is easily formed in reclamation projects, which triggers issues with the bearing capacity and nonuniform settlement of calcareous sand foundations. In this study, a series of one-dimensional compression tests were conducted to investigate the effect of different fines contents (f_c) on the compression behavior of calcareous sand. The results show that at the same relative density (medium-density, D_r = 50%), the addition of fine particles leads to a reduction in the initial void ratio (for $f_c \leq 40\%$). Furthermore, while the compressibility of the soil samples increases with the rising of fines content, it begins to decrease with further addition of fine particles beyond a threshold value of fines content ($f_{c\text{-th}}$). Additionally, particle crushing contributes to the compressive deformation of calcareous sand, and the particle relative breakage of calcareous sand increases at the initial stage of adding fine particles. Moreover, a comparison of the compression test results between calcareous silty sand (f_c = 10%) and clean sand reveals that the addition of fine particles accentuates the compressibility differences among calcareous sands with different relative densities. These findings provide valuable insights for addressing the challenges posed by fine-grained layers in calcareous sand foundations.

Keywords: calcareous sand; fines content; relative density; initial void ratio; compressibility; particle breakage; interparticle contact

Citation: Huang, S.; Gong, X. Effect of Fines Content on the Compression Behavior of Calcareous Sand. *Appl. Sci.* **2024**, *14*, 10457. https://doi.org/10.3390/app142210457

Academic Editor: Tiago Miranda

Received: 30 September 2024
Revised: 5 November 2024
Accepted: 7 November 2024
Published: 13 November 2024

1. Introduction

Coral reef sediments dominated by calcareous sand are found throughout the world. In recent decades, with the progressive extension of construction works into the oceanic areas, marine projects involving calcareous sand have developed rapidly (e.g., filling by hydraulic suction dredgers). Calcareous sand, the primary foundation material for marine construction and renovation projects, is a unique geotechnical medium formed by marine organisms, with a calcareous carbonate content exceeding 50%. Due to its unique formation process, calcareous sand exhibits special engineering characteristics such as irregular shape, high intra-grain porosity, high angularity, low particle hardness, and significant particle breakage, which leads to considerable differences in the basic mechanical properties compared to general terrestrial sands [1–6]. In addition, the hydraulic sorting effect during the blow-fill process causes uneven particle distribution in calcareous sand foundation, often resulting in the formation of fine-grained aggregation layers predominantly composed of fine sand with varying fines content. Consequently, calcareous sand foundation always has issues with insufficient bearing capacity and uneven settlement.

Scholars, both domestically and internationally, have explored the mechanisms by which fines content affects the mechanical properties of sandy soils. Thevanayagam et al. introduced the concepts of intergranular void ratio and inter-fine void ratio and proposed that significant microstructural changes occurred once the fines content in sandy soil surpasses a certain threshold, resulting in noticeable macroscopic mechanical differences among clean sands, silty sands, and sandy silts [7,8]. Lade et al. systematically examined how varying fines content affected the static liquefaction potential under monotonic compression

loading for Nevada sand and Ottawa sand. Their experimental findings demonstrated that increasing fines content enhanced the liquefaction potential of clean sand, with fine particles increasingly dominating the overall behavior of undrained soils after a certain fines content threshold was reached [9]. Zhou et al. conducted dynamic triaxial tests on undisturbed soil samples with varying fines content, finding that liquefaction resistance initially decreased and then increased as fines content rose. This shift was attributed to changes in the role of fine particles in the soil's load-bearing structure [10]. Based on the inter-grain contact index, Yin et al. proposed an elastoplastic model to effectively predict the mechanical behavior of sand–silt mixtures [11]. Shi et al. introduced a compression model for sand–marine clay mixtures within a homogenization framework [12]. Later, Shi et al. developed a simple and effective compression model for clay and silty sand, based on the concept of an equivalent void ratio [13]. Bouri et al. examined the effect of fines content on the compressibility of high-density Chelf sand (at relative densities of 65% and 80%), finding that the fines content transition depended on the initial state of the samples—such as relative density, preparation method, and maximum void ratio—and can be calculated using a hypoplastic model [14]. Recently, Hang et al. expanded the intergranular contact state classification for sand–fines mixtures proposed by Thevanayagam, introducing critical intergranular contact state parameters ($FC_{\text{in-min}}$ and $FC_{\text{in-max}}$) to characterize in-transition soils [15]. In summary, extensive research has been conducted on the influence of fines content on the mechanical properties of terrigenous sand, but studies in this area for calcareous sand remain insufficient. However, the above theoretical foundation of the microstructure of terrestrial sand–fine particles can provide a good reference for the study of mechanical properties of calcareous sand–fines mixtures.

Most studies have concentrated on the compressibility of terrigenous sand–silt mixtures [13,16–18], whereas researches on the compressibility of calcareous sand–silt mixtures are limited. Soil compression generally results from the reduction in pore volume, encompassing the compression of porous gas and the expulsion of pore water and gas. The deformation primarily stems from the compression of pore volume between soil particles. However, calcareous sand–silt mixtures may exhibit markedly different compressibility characteristics compared to quartz sand–silt mixtures. Coop and Liu conducted compression tests on calcareous sand from Dogs Bay in western Ireland and the South China Sea, respectively, and found that calcareous sand exhibited a higher compression coefficient [2,3]. The compression process in calcareous sand involves consolidation, particle rearrangement, and particle breakage, with this deformation being largely irreversible plastic deformation. This is because calcareous sand particles have a high internal porosity and tend to break at low stress levels [19,20]. Thus, it is crucial to account for both pore compression and particle breakage when evaluating the compressibility of calcareous sand. Through extensive laboratory testing, Zhang observed that calcareous sand initially underwent relative position changes between particles during compression, with volume reduction becoming increasingly dominated by particle breakage as pressure rose [21]. Other studies have similarly shown that particle breakage substantially enhanced the compressibility of calcareous sand [22–24]. Further research has explored the effects of various particle components on the compressibility of calcareous sand. Shi et al. conducted triaxial compression tests on coarse–fine particle mixtures with fines contents of 0%, 40%, and 60%, revealing that under low confining pressures, the sample volume decreased with increasing deviatoric stress, and higher fine content intensified volume shrinkage [25]. Qin et al. found that coarse particles can improve the compressibility of calcareous sand to some extent, concluding that the relatively most stable particle size during breakage was 0.25 mm [26]. Using quartz sand as a reference, Yang et al. examined the influence of gradation on calcareous sand's compressibility, showing that the compressibility of calcareous sand was significantly greater, and the coarse fraction (i.e., 1–5 mm) content has the most pronounced impact [5]. When the coarse fraction content is below 25%, and the mass ratio of medium to fine grains is constant, the most unfavorable coarse fraction content is reached, making calcareous sand highly compressible. Tian et al. studied the effects of gradation characteristics and

morphology on the compressibility and breakage of calcareous sand under high stress levels, finding that the compression curves of differently graded calcareous sands converge on the *e*-log *p* plane as vertical stress increased [6]. However, research on the impact of fines content on the compressibility of calcareous sand, particularly in the 0–40% range, remains limited.

In this study, laboratory experiments and mechanistic analyses on clean sand and calcareous silty sand with varying fines contents were conducted. The aim of this study was to explore the effects of fines content and initial relative density on the compressibility behavior of calcareous sand–fines mixture, and further investigate the particle breakage characteristic of calcareous silty sand and clean sand. Using a soil classification system based on inter-particle contacts, this study analyzed the intrinsic mechanism of how fines content affects the compressibility behavior of calcareous sand from a microstructural perspective. In addition, the threshold fines content ($f_{c\text{-}th}$) that signifies changes in the compressibility of calcareous sand is identified. The investigation of the impact of fines content on the mechanical properties of calcareous sand holds substantial engineering significance and offers broad application potential, particularly for addressing foundation issues caused by fine-grained aggregation layers.

2. Materials and Methods

2.1. Test Materials

The calcareous sand used in this study was sourced from an island reef in the South China Sea. Prior to testing, the calcareous sand was cleaned and dried. Then, it was sieved using nine different sieve layers: <0.075 mm, 0.075–0.01 mm, 0.1–0.15 mm, 0.15–0.25 mm, 0.25–0.355 mm, 0.355–0.5 mm, 0.5–1 mm, 1–2 mm, and 2–5 mm, to obtain calcareous sand particles of different sizes (see Figure 1). The large particle group of in situ calcareous sand (particle size > 2 mm) retained some skeletal forms of marine organisms, containing numerous irregular particles with branch-like and angular shapes. As the large particle group constituted less than 5% of the total mass, to minimize random errors, the study followed established practices by removing calcareous gravel larger than 2 mm, and focused on particles smaller than or equal to 2 mm. The particle size distribution curve of the remaining material is shown in Figure 2. The calcareous sand used in this study was unconsolidated granular material, with its detailed physical parameters provided in Table 1. The sample contained almost no fine particles smaller than 0.1 mm, with a uniformity coefficient of 2.5 and a curvature coefficient of 0.96, classifying it as poorly graded sand.

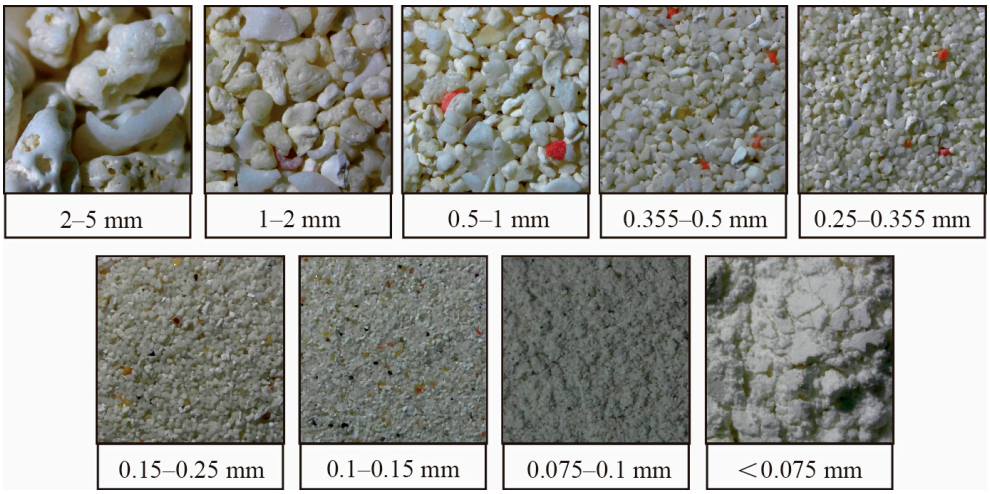

Figure 1. Calcareous sand particles with different grain sizes (same magnification).

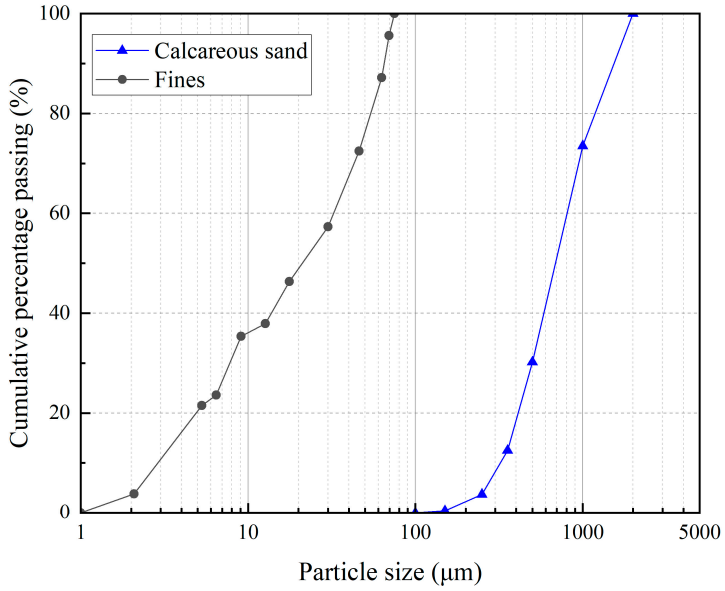

Figure 2. Particle size distribution curves of calcareous sand sample and fines.

Table 1. Basic physical parameters of the test material.

Test Material	G_s	d_{50} (mm)	d_{10} (mm)	d_{30} (mm)	d_{60} (mm)	C_u	C_c
Calcareous sand	2.78	0.69	0.32	0.50	0.81	2.5	0.96

The original calcareous sand was crushed into fine particles with diameters ranging from 1 to 75 μm, and its particle size distribution curve was determined using the hydrometer method (Figure 2). Subsequently, pure sand and the crushed fine material were uniformly mixed in varying dry weight ratios of 10:0, 9.5:0.5, 9:1, 8.5:1.5, 8:2, 7:3, and 6:4, resulting in seven soil samples: X-0, X-5%, X-10%, X-15%, X-20%, X-30%, and X-40%. The relative density tests were conducted in accordance with the "Standard for Soil Test Methods" (GB/T50123-2019) [27]. The minimum dry density was determined using both the funnel method and measuring cylinder method, with the smaller value (from the measuring cylinder method) selected. For the maximum dry density, the vibrating hammer method was used, employing a 250 mL compaction cylinder. These tests yielded the minimum and maximum dry densities of the seven soil samples, and the corresponding maximum and minimum void ratios were calculated using Equations (1) and (2) [27]. Table 2 presents the key physical parameters of these seven calcareous sand samples.

$$e_{max} = \frac{\rho_w G_s}{\rho_{dmin}} - 1 \quad (1)$$

$$e_{min} = \frac{\rho_w G_s}{\rho_{dmax}} - 1 \quad (2)$$

Table 2. Main physical properties of calcareous sand samples with varying fines contents.

Soil Samples	f_c	G_s	d_{50} (mm)	ρ_{dmin} (g/cm^3)	ρ_{dmax} (g/cm^3)	e_{max}	e_{min}
X-0	0	2.78	0.69	1.23	1.63	1.26	0.71
X-5%	5%	2.78	0.66	1.30	1.72	1.14	0.62
X-10%	10%	2.78	0.63	1.32	1.81	1.10	0.54
X-15%	15%	2.78	0.60	1.34	1.89	1.07	0.47
X-20%	20%	2.78	0.56	1.36	1.98	1.05	0.40
X-30%	30%	2.78	0.48	1.37	2.11	1.03	0.36
X-40%	40%	2.78	0.38	1.39	2.18	1.01	0.34

2.2. Method of One-Dimensional Compression Tests

The experimental setup employed a WG type single-lever consolidation apparatus, with sample dimensions of 61.8 mm in diameter and 20 mm in height. Weights were used to apply the load following this sequence: 5 kPa → 12.5 kPa → 25 kPa → 50 kPa → 100 kPa → 200 kPa → 400 kPa → 800 kPa → 1600 kPa. Vertical compression deformations were measured using a dial gauge with an accuracy of 0.01 mm. In its natural state, the relative density of calcareous sand ranges from 20% to 80%, predominantly in a medium dense state. Considering practical engineering conditions, the initial relative density of the calcareous sand samples in Test Series I was controlled at D_r = 50% (medium dense). Test Series II investigated the effect of adding fine particles on the compression characteristics of calcareous sand under different initial relative densities—low-density (D_r = 30%), medium-density (D_r = 50%), and high-density (D_r = 70%). The initial void ratio (e_0) of each sample can be determined from Equation (3) [27]. The test scheme is detailed in Table 3.

$$D_r = \frac{e_{max} - e_0}{e_{max} - e_{min}} \tag{3}$$

Table 3. Test scheme for calcareous sand samples with varying fines contents.

Test Series	Test No.	Soil Samples	f_c	D_r	e_0
I	A	X-0	0	50%	0.985
	B	X-5%	5%		0.880
	C	X-10%	10%		0.820
	E	X-15%	15%		0.770
	F	X-20%	20%		0.725
	G	X-30%	30%		0.693
	H	X-40%	40%		0.673
II	I	X-0	0	30%	1.095
	A			50%	0.985
	J			70%	0.875
	K	X-10%	10%	30%	0.932
	C			50%	0.820
	L			70%	0.708

2.3. Relative Breakage Model

To evaluate the degree of particle breakage, the relative breakage model proposed by Hardin was employed [28], as shown in Figure 3. This model, which tracks changes in particle size distribution before and after testing, is widely applied in quantitatively assessing the extent of particle breakage. The theory assumes that all particles will break into fine grains under sufficiently large loads, thus defining 0.074 mm as the limiting particle size that can undergo breakage. Consequently, this study used the relative breakage (B_r) as the indicator for evaluating the degree of particle breakage. The Equation (4) is as follows:

$$B_r = \frac{B_t}{B_p} = \frac{S_{ABEFD}}{S_{ACFD}} \tag{4}$$

where B_t represents total breakage potential, defined by the area enclosed between the particle size distribution curves before and after breakage and the vertical line at d = 0.074 mm; B_p denotes the initial breakage potential, defined by the area enclosed between the particle size distribution curve before breakage and the vertical line at d = 0.074 mm.

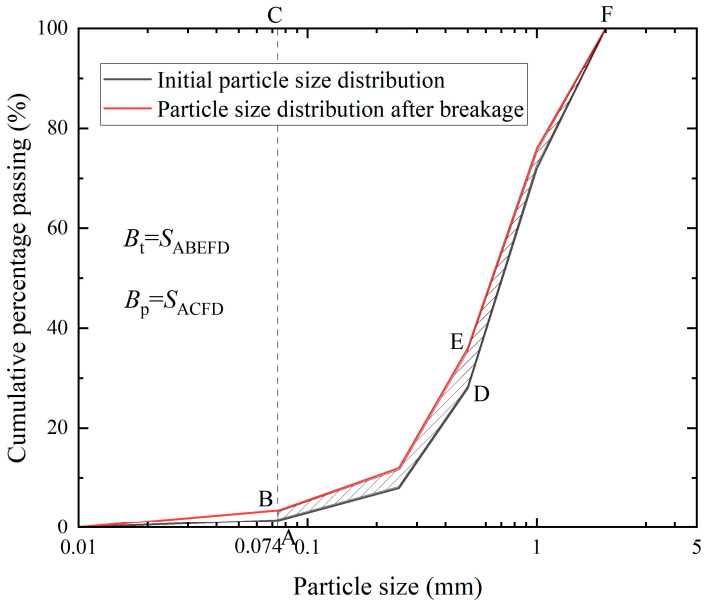

Figure 3. Schematic diagram of the relative breakage model.

3. Results of Compression Tests

3.1. Effects of Fines Content on the Initial Void Ratio and Compression Characteristics of Calcareous Sand

Test Series I investigated the one-dimensional compression behavior of calcareous silty sand and clean sand at a consistent initial relative density (D_r = 50%, medium dense).

Figure 4 presents the *e*-log *p* compression curves for calcareous sand samples with varying fines contents. Figure 5 displays the relationships between the compression coefficient ($a_{1\text{-}2}$) and the initial void ratio (e_0) with varying fines contents (f_c). The compression coefficient in this study was examined within a pressure range of100–200 kPa (as shown in Figure 3). Across the fines content range studied ($0 \leq f_c \leq 40\%$), substantial differences in the initial void ratios of the calcareous sand samples were observed. As fines content increased, the initial void ratio gradually decreased from 0.985 to 0.673. This reduction can be attributed to the particle morphology of calcareous sand: the original sand had well-developed angular features and irregular particle shapes that easily interlocked and created voids, resulting in a high initial void ratio. However, as fine particles were added, some of these voids were gradually filled, leading to a decrease in the initial void ratio. As illustrated in Figure 5, the compression coefficient of samples with varying fines content ranged from 0.079 to 0.119. The compression coefficient initially increased and then decreased as the fines content increased. According to the compression classification criteria for soils, Sample A, B, C, and H (f_c = 0%, 5%, 10%, 40%) were classified as low-compressibility soils, while Sample E, F, and G (f_c = 15%, 20%, 30%) were classified as medium-compressibility soils. Notably, the compression coefficient of Sample B (f_c = 5%) was similar to that of the clean sand (Sample A), indicating that the addition 5% fine particles has a minimal impact on compressibility of calcareous sand. However, the compressibility of Sample C (f_c = 10%) increased by 18.2% compared to Sample A (as represented by $a_{1\text{-}2}$), suggesting that a fines content of 10% or higher significantly alters the compression coefficient.

Figure 6 presents the curves depicting the vertical compression deformation percentages of Sample A–H under varying axial loads as a function of fines content. It is evident that within the considered range of fines content, the calcareous silty sand Sample E (f_c = 15%) exhibits greater vertical strain under all levels of load compared to the other samples. The trend of axial deformation follows a distinct "∩"-shaped curve, where deformation increases with rising fines content, peaks at 15%, and then gradually decreases. At approximately 15% fines content, the calcareous silty sand enters a transitional phase, during which the sample exhibits the maximum compression deformation. Under an

axial load of 1600 kPa, samples with fines contents of 15% and 20% show the maximum compression deformation, reaching up to 5.7%. Particularly at low consolidation stresses (i.e., less than 600 kPa), the influence of fines content on the compression performance of calcareous sand is more pronounced.

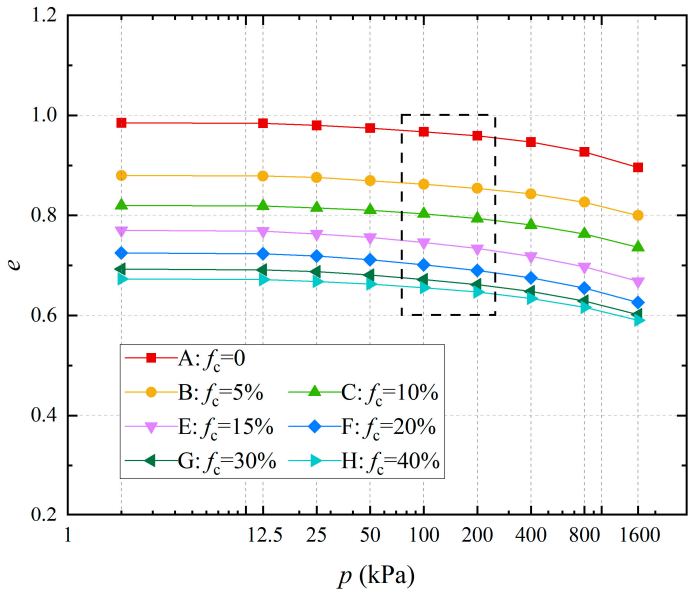

Figure 4. *e*-log *p* curves for calcareous sand samples with varying fines contents (D_r = 50%). *e*: void ratio.

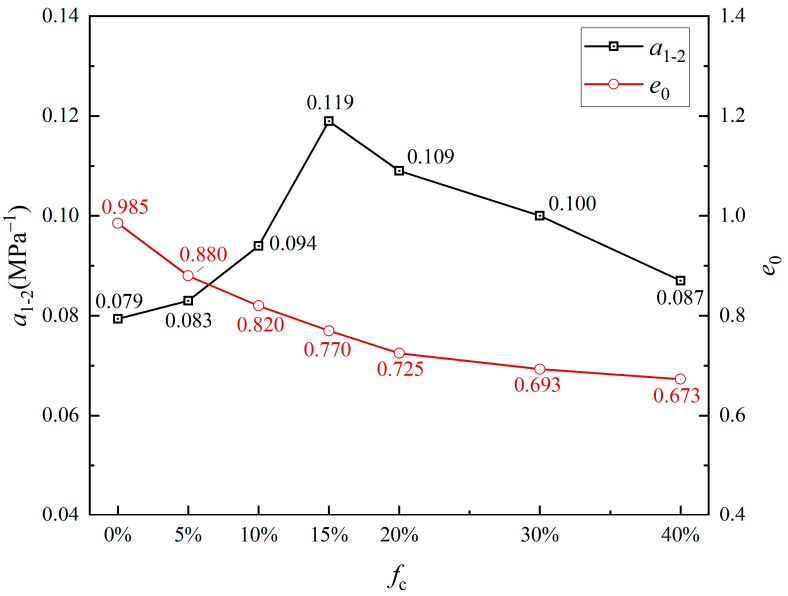

Figure 5. The relationship between compression coefficient and initial void ratio of calcareous sand with varying fines contents (D_r = 50%).

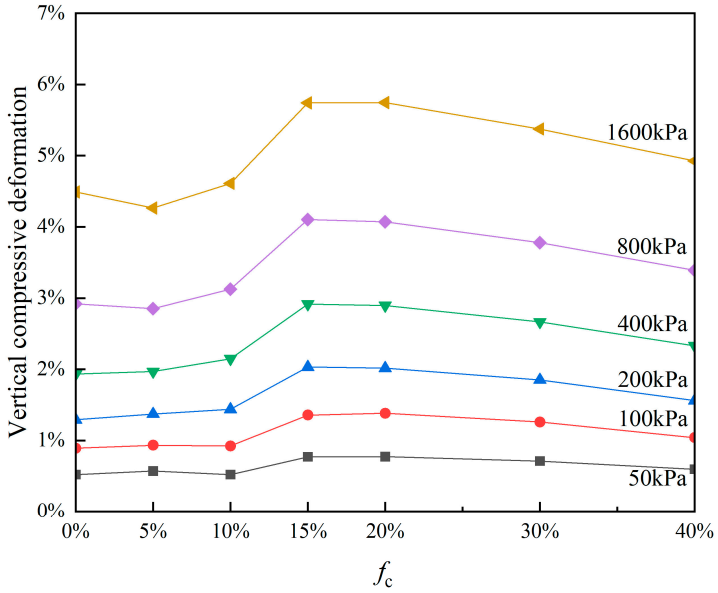

Figure 6. Vertical compression deformation with varying fines contents under different levels of axial load (D_r = 50%).

Figure 7 illustrates the variation of the coefficient of volumetric compressibility (m_v) for Sample A–H as a function of fines content (f_c) under various axial loads. From Figure 7a, it is observed that the coefficient of volumetric compressibility of each sample decreases with the increase in axial load. At low stress levels, the coefficient of volumetric compressibility is strongly influenced by the fines content, whereas this effect diminishes under higher stress levels. Figure 7b describes the relationship between the coefficient of volumetric compressibility and fines content under vertical stresses of 100 kPa, 200 kPa, 400 kPa, 800 kPa, and 1600 kPa. It is clear that the compressibility of Sample E and F (with f_c = 15% and 20%, respectively) is significantly higher than that of other samples. For the calcareous material studied, total compressibility is highest when the fines content ranges from 15% to 20%, indicating that the calcareous silty sand is in a transitional state within this range.

3.2. Effects of Fines Content on Compression Characteristics of Calcareous Sand at Different Initial Relative Density States

Test Series II compared calcareous silty sand with a fine particle content of 10% (soil sample X-10%) to clean sand, examining the impact of adding fine particles on the compressibility of calcareous sand at various initial relative densities (low-density D_r = 30%, medium-density D_r = 50%, high-density D_r = 70%). The soil sample X-10% was selected based on the results from Test Series I, which demonstrated that when the fines content reached 10%, the effect of fine particle addition on the compressibility of calcareous silty sand became significantly more evident. Figure 8 presents the variation in the coefficient of volumetric compressibility (m_v) with axial load for both clean sand and calcareous silty sand (f_c = 10%) across three different relative densities. The figure demonstrates that, regardless of whether the sand is clean or mixed, a higher initial relative density leads to a lower volume compression coefficient and reduced compressibility. The results further reveal that, under low- and medium-density conditions, the addition of fine particles increases the coefficient of volumetric compressibility, while under high-density conditions, it decreases the coefficient. Furthermore, the differences in the coefficients of volumetric compressibility among the silty sand Sample K, C, and L (D_r = 30%, 50%, 70%) are significantly greater than those among the clean sand Sample I, A, and J (D_r = 30%, 50%, 70%). For example, under a vertical load of 400 kPa, the coefficient difference of volumetric compressibility between clean sand Sample I (D_r = 30%) and J (D_r = 70%) is 0.8 × 10^{-5}/kPa, while the difference between mixed sand Sample K (D_r = 30%) and L (D_r = 70%) is 1.8 × 10^{-5}/kPa.

This phenomenon indicates that the addition of fine particles amplifies the compressibility differences between samples with varying initial relative densities.

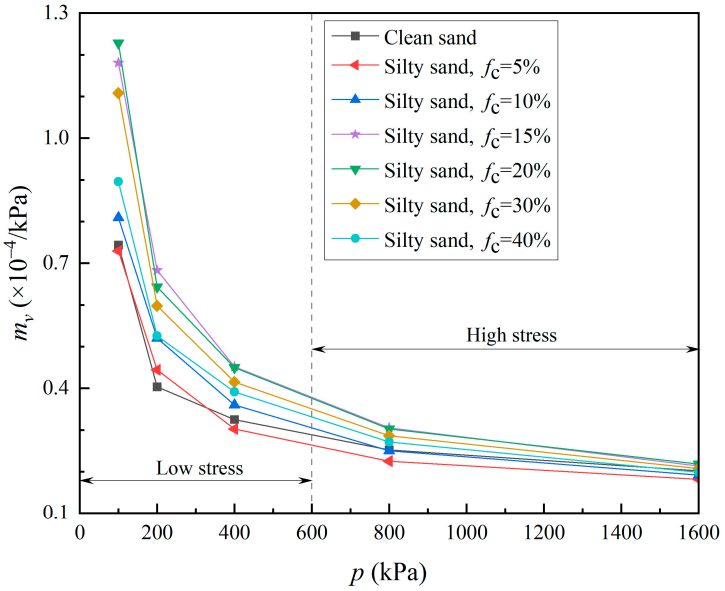

(**a**) Variation of the coefficient of volumetric compressibility of each sample with axial load

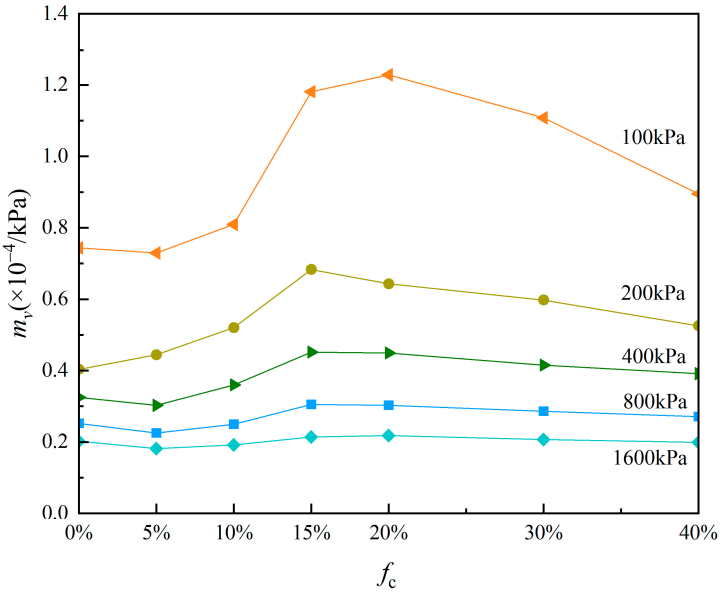

(**b**) Variation of the coefficient of volumetric compressibility with fines contents

Figure 7. Variation of the coefficient of volumetric compressibility with varying fines contents under different levers of axial load (D_r = 50%).

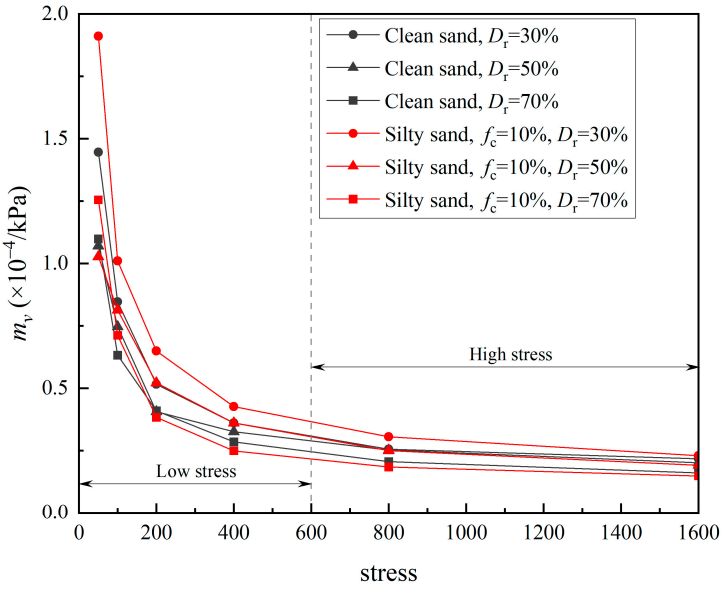

Figure 8. The variation of the coefficient of volumetric compressibility of clean sand and mixed sand samples with axial load under different initial relative densities.

3.3. Effects of Fines Content on the Particle Breakage Characteristics of Calcareous Sand

For mixed soils containing calcareous sand, particle breakage leads to significant volumetric reduction [29–31]. Shahnazari et al. found that for Persian Gulf calcareous sand under pressures below 1000 kPa, up to 20% of the total axial strain is attributed to particle breakage [32]. This volumetric change is driven by two factors: the re-arrangement of particles following breakage, which reduces the overall void ratio of the sand skeleton [33], and the release of intra-particle voids after breakage, which provides additional space for fine sand particles. Therefore, the volumetric reduction associated with particle breakage also contributes to the compressive deformation of calcareous sand.

Through Equation (4), it is evident that the relative breakage (B_r) ranges between 0 and 1, where a value closer to 1 indicates a more severe degree of particle breakage. Using the aforementioned calculation method and the particle size distribution curves before and after compression testing, the relative breakage for Sample A–H were calculated, with results presented in Table 4. It can be observed that in the initial stage of adding fines, the relative breakage of calcareous sand increases, especially the Br value of calcareous silty sand Sample C is 2.44 times that of Sample A. This phenomenon indicates that under the same loading path, the stress required for significant breakage occurs earlier with the addition of fine particles. Furthermore, when the stress levels are equal, the amounts of breakage for Sample B, C, E, and F significantly increase with the addition of fines. It can be explained by the particle shape characteristics and the development of internal voids in calcareous sand. On one hand, during compression, the average contact area between the irregularly shaped coarse particles of calcareous sand is relatively small, making it easier to form high localized stress at these contact points or surfaces, which causes particle breakage. With the addition of fines, the number of particles in contact around each coarse particle decreases, increasing the average stress acting on that coarse particle, thus making breakage more likely. On the other hand, the addition of fine particles causes point contacts between coarse particles to deviate from the centroid, generating additional bending moments on the particles, and making stress concentration more likely to occur at their smaller size directions and irregular contact points (corner contact points), thereby exacerbating breakage ($B_{r\text{-}C} > B_{r\text{-}B} > B_{r\text{-}A}$). The small particles formed from the breakage of coarse particles fill the voids between them, reducing the void ratio while releasing internal voids, which further increases the compressive deformation of the samples. However, as the fines content increases further, the load-bearing soil framework gradually transitions to being supported by both coarse and fine particles. As a result, the aforementioned two effects of

particle breakage caused by fines weaken, leading to a reduction in the relative breakage of the samples ($B_{r\text{-}H} < B_{r\text{-}F} < B_{r\text{-}C}$). The phenomenon of particle breakage of calcareous sand further clarifies the results of the compression tests mentioned above. At higher stress levels, in the initial stage of adding fines (Sample B–F), the degree of particle breakage increased, which contributed to the compressive deformation of the samples. However, as the fines content increased further (Sample G and H), the degree of particle breakage relatively decreased, thereby playing a mitigating role in the compression deformation of the samples.

Table 4. The particle breakage results of samples.

Sample	f_c	e_0	$a_{1\text{-}2}$	B_r
A	0	0.985	0.079	0.18%
B	5%	0.880	0.083	0.29%
C	10%	0.820	0.094	0.44%
E	15%	0.770	0.119	0.36%
F	20%	0.725	0.109	0.24%
G	30%	0.693	0.100	0.17%
H	40%	0.673	0.087	0.13%

4. Soil Framework and Compressibility Behavior Analysis

Building on an intergranular contact state classification method [34], this paper considers calcareous silty sand samples as particle mixtures containing particles of sizes D (original calcareous sand particles) and d (added fines) in different proportions. A detailed microstructural analysis of these mixtures is provided, along with an investigation of how varying fines content influences the compressive behavior of calcareous silty sand (Figure 9). Four distinct microstructural configurations were identified as follows: (i) a framework entirely composed of coarse particles (Sample A); (ii) coarse particles mainly in contact, with fine particles filling voids and providing minimal support (Sample B); (iii) coarse particles still in contact, but fine particles begin to contribute to the framework's support (Sample C, E, F); and (iv) fine particles are in contact, completely isolating the coarse particles (Sample G, H). Sample A to H undergo a transition from case (i) to case (iv) at the microstructural level. The transition from Sample A to H reflects a shift from case (i) to (iv), indicating that as fines content increases, the microstructure evolves, with a threshold fines content ($f_{c\text{-}th}$) occurring between cases (iii) and (iv). Based on compression test results, the threshold fines content ($f_{c\text{-}th}$) for calcareous silty sand is approximately 15–20% (medium-density, D_r = 50%). When f_c is less than $f_{c\text{-}th}$, particularly in Sample B, C, E, and F (f_c = 5%, 10%, 15%, and 20%), the microstructure is dominated by coarse particle contacts, forming the load-bearing skeleton, with fine particles playing a minor role. However, when f_c exceeds the threshold $f_{c\text{-}th}$, as seen in Sample G and H (f_c = 30% and 40%), the microstructure transitions to case (iv), where fine particles dominate the load-bearing structure.

The above compression test shows that the addition of 5% fine particles has a minimal effect on compressibility. Furthermore, it is evident that as the fines content increases, the axial deformation first rises and then declines. This behavior can be explained using the classification method based on the inter-particle contact state. Given that the added fines (d < 75 μm) are much smaller than the diameter of the original calcareous sand particles (D), and that the fines only partially fill the voids between coarse particles without fully occupying them, the microstructure of Sample B (f_c = 5%) closely resembles case (i). In Sample B, C, E, and F (f_c = 5%, 10%, 15%, and 20%), the load-bearing skeleton is primarily supported by coarse particles, while fine particles play a secondary role. The interlocking of coarse particles forms a relatively stable skeleton, but with the addition of fines, the fine particles act as lubricants between the coarse particles, reducing the skeleton's stability and promoting particle rearrangement, leading to increased axial deformation under the same load. As the fines content continues to increase, as observed in Sample G and H

(f_c = 30% and 40%), the coarse particles within the load-bearing soil skeleton are progressively replaced by fine particles. This reduces the likelihood of particle rearrangement, consequently lowering axial deformation and compressibility.

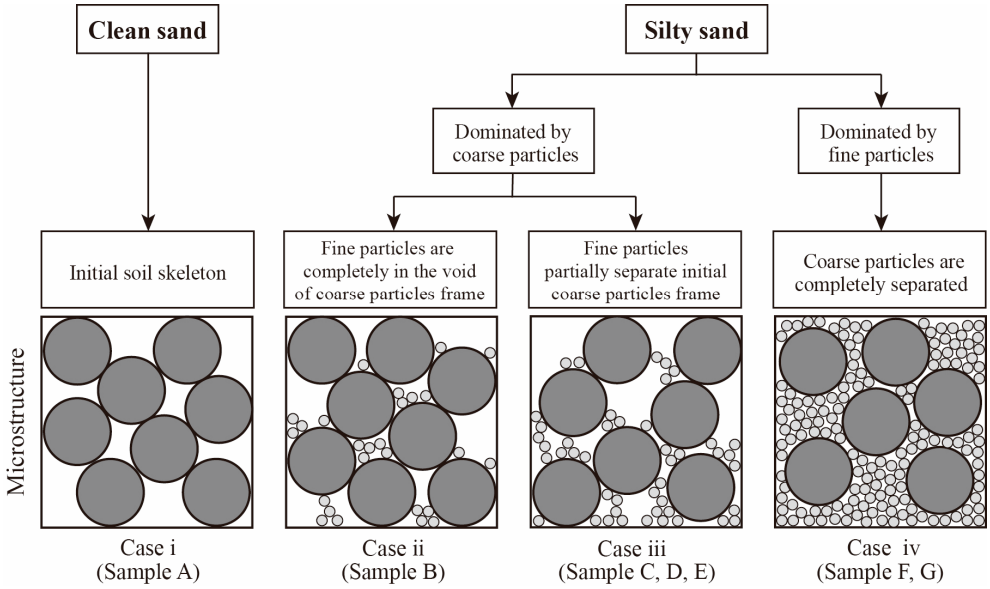

Figure 9. Interparticle contact state classification for calcareous clean sand and silty sand.

In the Series II tests, the microstructures of Sample I (low-density, D_r = 30%), A (medium-density, D_r = 50%), and J (high-density, D_r = 70%) all correspond to case (i), where the load-bearing framework is entirely composed of original calcareous sand particles. For these samples, higher initial relative density leads to a smaller initial void ratio and fewer voids between particles, consequently resulting in lower compressibility. Sample K (low-density, D_r = 30%), C (medium-density, D_r = 50%), and L (high-density, D_r = 70%), made from the soil sample X-10%, exhibit the same trend: increased initial relative density corresponds to a reduced void ratio and decreased compressibility. The microstructure of low-density Sample K, similar to that of medium-density Sample C, aligns with case (iii), where coarse particles predominantly contact each other. Adding fines facilitates particle rearrangement, increasing axial deformation under the same load. Conversely, the microstructure of high-density Sample L aligns more closely with case (iv), where the load-bearing framework is primarily supported by fine particles, and the addition of fines reduces compressibility. These observations suggest that the threshold of fines content ($f_{c\text{-}th}$) shifts depending on the relative density: it occurs earlier in high-density samples and later in low-density samples compared to medium-density samples.

5. Discussion

With the increasing expansion of land reclamation projects, the issue of the fine-grained aggregation layers in calcareous sandy soil affecting the foundation's bearing performance has gained prominence. In this study, the compressibility differences between calcareous fine sand with different fine particle contents and clean sand were studied in detail.

The comprehensive analysis revealed that at a medium-density state (D_r = 50%), the axial deformation trend displays a distinct "∩" shape with an increase in fines content, depicted in Figure 5. Similarly, the coefficient of volumetric compressibility (m_v) of calcareous sand samples exhibits an initial increase followed by a decrease, shown in Figure 6. It can be concluded that when the fines content is between 15% and 20%, the compression behavior of calcareous sand–fines mixture is in a transitional state. From a microscopic perspective, as fine particles are continuously added, the load-bearing soil structure shifts from being primarily composed of original calcareous sand particles to being dominated by fine particles, as demonstrated in Figure 9. This study suggests that the fines content

threshold ($f_{c\text{-}th}$) is approximately 15–20%, which indicates the compressibility changes in powdery calcareous sand. Furthermore, variations in the initial relative density influence the value of $f_{c\text{-}th}$ timing, with a higher density leading to an earlier threshold appearance and lower density delaying it. In addition, a comparison of particle breakage was carried out. It is worth noting that the particle relative breakage of calcareous sand increases at the initial stage of the addition of fine particles.

Previous research on the compression behavior of calcareous sand mostly concentrated on coarse particle components [5,26], and limitations in the selection of fines content for studying the compressibility of calcareous silty sand persist [25]. In this study, the compression behavior of calcareous sand–fines mixtures across the 0–40% fines content range can be supplemented in more detail. The results can offer valuable insights for addressing calcareous soil foundation bearing capacity challenges caused by the fine-grained aggregation layer during land reclamation projects. Furthermore, notable differences exist in the shear mechanical properties between calcareous sand and quartz sand [6,35]. Subsequent research directions could investigate the impact of fines content on the shear mechanical properties of calcareous sand–fines mixtures, especially focusing on the correlation between the fines content threshold reflecting shear changes and the initial state of calcareous sand.

6. Conclusions

In this study, the one-dimensional compression behavior of clean sand and calcareous silty sand with varying fines contents was investigated. The effects of fines content and initial relative density on compression and particle breakage characteristics were examined. Additionally, the intrinsic mechanisms of how fines content affects the compressibility behavior of calcareous sand were analyzed from a microstructural perspective. The main conclusions are summarized as follows:

(1) Under identical initial relative density conditions (D_r = 50%), the initial void ratio of calcareous silty sand samples decreased progressively with the increase in fines content. The compression coefficient ($a_{1\text{-}2}$) of these samples ranged from 0.079 to 0.119, showing a pattern of initial increase followed by a decrease with the increase in fines content, indicating a transition from low-compressibility soil to medium-compressibility soil, and eventually back to low-compressibility soil.

(2) Under the same gradation and density conditions, the addition of 5% fines had minimal impact on the compressibility of calcareous sand. However, when the fines content reached 10% or more, the compression coefficient underwent significant changes.

(3) In the initial stages of adding fines, the relative breakage of calcareous sand significantly increased, especially the Br value of silty sand Sample C was three times that of clean sand Sample A.

(4) As fines content increased, the volumetric coefficient (m_v) of calcareous sand samples showed a tendency to initially increase and then decrease. This behavior is attributed to two factors as follows: first, the reorganization of particle arrangement influenced by inter-particle contact, and second, the volume reduction caused by particle breakage. As fines content rises, the microstructure of calcareous silty sand shifts from coarse particle-to-particle contact to fine particle-to-particle contact. The threshold fine content ($f_{c\text{-}th}$) reflecting changes in the compressibility of calcareous silty sand is approximately 15–20% at medium-density (D_r = 50%).

(5) The addition of fine particles exacerbates compressibility differences between calcareous sands with varying relative densities. The threshold fines content ($f_{c\text{-}th}$) for calcareous sands with different relative densities also varies. In comparison to medium-density samples, $f_{c\text{-}th}$ appears earlier in high-density samples and later in low-density samples.

Author Contributions: Conceptualization, S.H.; data curation, S.H.; formal analysis, S.H.; methodology, S.H.; funding acquisition, X.G.; investigation, S.H.; software, S.H.; project administration, S.H. and X.G.; resources, S.H. and X.G.; supervision, S.H.; validation, S.H.; visualization, S.H.; writing—original draft, S.H.; writing—review and editing, S.H. All authors have read and agreed to the published version of the manuscript.

Funding: This research was funded by National Natural Science Foundation of China (51778575).

Institutional Review Board Statement: Not applicable.

Informed Consent Statement: Not applicable.

Data Availability Statement: The data presented in this study are available on request from the corresponding author. The raw/processed data needed to reproduce these findings cannot be shared publicly at this time, as they are also part of ongoing study.

Conflicts of Interest: The authors declare no conflicts of interest.

Nomenclature

$a_{1\text{-}2}$	compression coefficient
B_r	relative breakage
C_c	curvature coefficient
C_u	uneven coefficient
D_r	relative density
d_{10}	effective size, particle size when the cumulative percentage of mass of soil particles less than a certain particle size is 10%
d_{30}	particle size when the cumulative percentage of mass of soil particles less than a certain particle size is 30%
d_{50}	average particle size, particle size when the cumulative percentage of mass of soil particles less than a certain particle size is 50%
d_{60}	constrained particle size, particle size when the cumulative percentage of mass of soil particles less than a certain particle size is 60%
e_0	initial void ratio
e_{max}	maximum void ratio
e_{min}	minimum void ratio
f_c	fines content
$f_{c\text{-}th}$	threshold fines content
G_s	specific gravity of calcareous sand
m_v	coefficient of volumetric compressibility
p	axial load
ρ_{dmax}	maximum dry density
ρ_{dmin}	minimum dry density
ρ_w	density of water

References

1. Fahey, M. The response of calcareous soil in static and cyclic triaxial tests. In *Engineering for Calcareous Sediments*; CRC Press: Boca Raton, FL, USA, 1988; Volume 1.
2. Coop, M.R. The mechanics of uncemented carbonate sands. *Géotechnique* **1990**, *40*, 607–626. [CrossRef]
3. Liu, C.Q.; Wang, R. Preliminary research on physical and mechanical properties of calcareous sand. *Rock Soil Mech.* **1998**, *19*, 32–37. [CrossRef]
4. Altuhafi, F.N.; Coop, M.R. Changes to particle characteristics associated with the compression of sands. *Géotechnique* **2011**, *61*, 459–471. [CrossRef]
5. Yang, S.; Shen, X.; Liu, H.; Ge, H.; Rui, X. Gradation affects basic mechanical characteristics of Chinese calcareous sand as airport subgrade of reefs. *Mar. Georesour. Geotechnol.* **2020**, *38*, 706–715. [CrossRef]
6. Tian, C.Y.; Lan, H.X.; Liu, X. Study on compression and crushing mechanical properties of calcareous sand considering influence of morphology and grading. *J. Eng. Geol.* **2021**, *29*, 1700–1710. [CrossRef]
7. Thevanayagam, S. Effect of fines and confining stress on undrained shear strength of silty sands. *J. Geotech. Geoenviron. Eng.* **1998**, *124*, 479–491. [CrossRef]

8. Thevanayagam, S.; Mohan, S. Intergranular state variables and stress-strain behaviour of silty sands. *Géotechnique* **2000**, *50*, 1–23. [CrossRef]
9. Lade, P.V.; Yamamuro, J.A. Effects of nonplastic fines on static liquefaction of sands. *Can. Geotech. J.* **1997**, *34*, 918–928. [CrossRef]
10. Zhou, J.; Yang, Y.X.; Jia, M.C.; Wu, F. Effect of fines content on liquefaction properties of saturated silty sands. *J. Hydraul. Eng.* **2009**, *40*, 1184–1188. [CrossRef]
11. Yin, Z.Y.; Huang, H.W.; Hicher, P.Y. Elastoplastic modeling of sand-silt mixtures. *Soils Found.* **2016**, *56*, 520–532. [CrossRef]
12. Shi, X.S.; Yin, J. Experimental and theoretical investigation on the compression behavior of sand-marine clay mixtures within homogenization framework. *Comput. Geotech.* **2017**, *90*, 14–26. [CrossRef]
13. Shi, X.S.; Zhao, J. Practical estimation of compression behavior of clayey/silty sands using equivalent void-ratio concept. *J. Geotech. Geoenviron. Eng.* **2020**, *146*, 04020046. [CrossRef]
14. Bouri, D.E.; Brahimi, A.; Krim, A.; Arab, A.; Najser, J.; Mašín, D. Compression behaviour of chlef sand and transition of fines content using pressure-dependent maximum void ratios of sand. *Geotech. Geol. Eng.* **2022**, *40*, 1675–1692. [CrossRef]
15. Hang, T.; Wu, Q.; Wang, Z.; Cheng, K.; Li, L.; Chen, G. A new procedure for characterizing the critical intergranular contact state of non-plastic sand-fines mixed materials. *Case Stud. Constr. Mater.* **2024**, *20*, e02881. [CrossRef]
16. Watabe, Y.; Yamade, K.; Saitoh, K. Hydraulic conductivity and compressibility of mixtures of Nagoya clay with sand or bentonite. *Géotechnique* **2011**, *61*, 211–219. [CrossRef]
17. Hsiao, D.H.; Phan, V.T.A.; Hsieh, Y.T.; Kuo, H.Y. Engineering behavior and correlated parameters from obtained results of sand-silt mixtures. *Soil Dyn. Earthq. Eng.* **2015**, *77*, 137–151. [CrossRef]
18. Chu, C.; Wu, Z.; Deng, Y.; Chen, Y.; Wang, Q. Intrinsic compression behavior of remolded sand-clay mixture. *Can. Geotech. J.* **2017**, *54*, 926–932. [CrossRef]
19. Wang, X.Z.; Wang, X.; Jin, Z.C.; Meng, Q.S.; Zhu, C.Q.; Wang, R. Shear characteristics of calcareous gravelly soil. *Bull. Eng. Geol. Environ.* **2017**, *76*, 561–573. [CrossRef]
20. Wei, H.Z.; Zhao, T.; He, J.Q.; Meng, Q.; Wang, X. Evolution of particle breakage for calcareous sands during ring shear tests. *Int. J. Geomech.* **2018**, *18*, 04017153. [CrossRef]
21. Zhang, J.M. *Study on the Fundamental Mechanical Characteristics of Calcareous Sand and the Influence of Particle Breakage*; Institute of Rock and Soil Mechanics, Chinese Academy of Sciences: Wuhan, China, 2004.
22. Shen, J.H.; Wang, R. Study on engineering properties of calcareous sand. *J. Eng. Geol.* **2010**, *18*, 26–32.
23. Li, Y.B.; Li, S.; Liu, X.L.; Chen, W. Effect of particle breakage on compression properties of calcareous sands with oedometer tests. *J. Eng. Geol.* **2020**, *28*, 352–359. [CrossRef]
24. Liu, X.; Tian, C.Y.; Lan, H.X. Laboratory investigation of the mechanical properties of a rubber-calcareous sand mixture: The effect of rubber content. *Appl. Sci.* **2020**, *10*, 6583. [CrossRef]
25. Shi, J.; Wang, Y.; Fan, Y.L.; Li, K.; Xiong, Y. Study on mechanical characteristics of soil mixed with coarse and fine particles. *Northwest Hydropower* **2013**, *3*, 54–56. [CrossRef]
26. Qin, Y.; Yao, T.; Wang, R.; Zhu, C.Q.; Meng, Q.S. Particle breakage-based analysis of deformation law of calcareous sediments under high-pressure consolidation. *Rock Soil Mech.* **2014**, *35*, 3123–3128. [CrossRef]
27. *GB/T 50123-2019*; Standard for Geotechnical Testing Method. SAC: Beijing, China, 2019.
28. Hardin, B.O. Crushing of soil particles. *J. Geotech. Eng.* **1985**, *111*, 1177–1192. [CrossRef]
29. Kwag, J.M. Yielding stress characteristics of carbonate sand in relation to individual particle fragmentation strength. In *Engineering for Calcareous Sediments*; Al-Shafei, K.A., Ed.; AA Balkema: Rotterdam, The Netherlands, 1999; pp. 79–87.
30. Xiao, Y.; Liu, H.; Desai, C.S.; Sun, Y.; Liu, H. Effect of intermediate principal-stress ratio on particle breakage of rockfill material. *J. Geotech. Geoenviron. Eng.* **2016**, *142*, 06015017. [CrossRef]
31. Xiao, Y.; Long, L.; Matthew Evans, T.; Zhou, H.; Liu, H.; Stuedlein, A.W. Effect of Particle Shape on Stress-Dilatancy Responses of Medium-Dense Sands. *J. Geotech. Geoenviron. Eng.* **2019**, *145*, 04018105. [CrossRef]
32. Shahnazari, H.; Rezvani, R. Effective parameters for the particle breakage of calcareous sands: An experimental study. *Eng. Geol.* **2013**, *159*, 98–105. [CrossRef]
33. Chen, W.B.; Liu, K.; Feng, W.Q.; Borana, L.; Yin, J.H. Influence of matric suction on nonlinear time-dependent compression behavior of a granular fill material. *Acta Geotech.* **2020**, *15*, 615–633. [CrossRef]
34. Thevanayagam, S.; Martin, G.R. Liquefaction in silty soils—Screening and remediation issues. *Soil Dyn. Earthq. Eng.* **2002**, *22*, 1035–1042. [CrossRef]
35. Głuchowski, A.; Li, L.Z.; Iskander, M. Effect of compression and shear on particle breakage of silica and calcareous sands. *Acta Geotech.* **2024**, *19*, 1–27. [CrossRef]